Scientific Research Publishing

Journal of Water Resource and Protection, 2025, 17(6), 378-402
https://www.scirp.org/journal/jwarp
ISSN Online: 1945-3108
ISSN Print: 1945-3094

Groundwater Potential Mapping in the Sissili Sub-Catchment, Burkina Faso: Comparing Multicriteria Analysis and Artificial Intelligence in a Crystalline Basement Aquifer

Tatiana Stella Kiswendsida Yameogo[1,2], Martine Diallo/Kone[3], Ludwig Ralf[4], Benjamin Bonkoungou[2], Julien Adounkpe[1,5]

[1]Doctoral Research Program in Climate Change and Water Resources, Applied Hydrology Laboratory (LHA) National Water Institute, University of Abomey Calavi, Cotonou, Benin
[2]Competence Center, West African Science Service Centre on Climate Change and Adapted Land Use (WASCAL), Ouagadougou, Burkina Faso
[3]Institute for Research in Applied Sciences and Technology, Ouagadougou, Burkina Faso
[4]Physical Geography, Environmental Modelling and Geographic Remote Sensing Laboratory, Munich, Germany
[5]Laboratory of Applied Ecology, Faculty of Agricultural Sciences (FSA), University of Abomey-Calavi (UAC), Cotonou, Benin Republic
Email: yameogo.t@edu.wascal.org

How to cite this paper: Yameogo, T.S.K., Diallo/Kone, M., Ralf, L., Bonkoungou, B. and Adounkpe, J. (2025) Groundwater Potential Mapping in the Sissili Sub-Catchment, Burkina Faso: Comparing Multicriteria Analysis and Artificial Intelligence in a Crystalline Basement Aquifer. *Journal of Water Resource and Protection*, **17**, 378-402.
https://doi.org/10.4236/jwarp.2025.176019

Received: April 4, 2025
Accepted: June 9, 2025
Published: June 12, 2025

Abstract

Groundwater is an essential resource for rural dwellers in Burkina Faso, a country with limited surface water availability. However, localising and accessing groundwater is challenging. This research illustrates the use of Remote Sensing (RS), Geographic Information System (GIS), Analytical Hierarchical Process (AHP), and Artificial Neural Networks (ANN) to determine groundwater potential zones in the Sissili sub-basin. The AHP and ANN processes, using nine (9) selected factors affecting groundwater availability, were mapped and reclassified using a descriptive scale. The two maps obtained included five classifications: very low, low, moderate, high, and very high. The AHP model classified 16.36% (1236.43 km^2) as very low, 51.53% (3895.39 km^2) as low, 29.24% (2209.89 km^2) as moderate, 2.82% (213.17 km^2) as high and 0.05% (4.12 km^2) as very high. For very low, low, moderate, high, and very high, the ANN model classified 43.56% (3292.98 km^2), 14.60% (1103.82 km^2), 31.10% (2350.86 km^2), 9.10% (687.82 km^2), and 1.63% (123.52 km^2) of the area respectively. The results were validated using the borehole yield and the Area Under the Curve (AUC). The ANN map results have demonstrated higher accuracy, becoming the most suitable groundwater potential zone delineation method.

Keywords

Analytical Hierarchy Process, Artificial Neural Network, Groundwater Potential Zones, Remote Sensing, Sissili Sub-Catchment

1. Introduction

Groundwater is a vital component of life on Earth and makes up nearly all of the world's liquid freshwater (over 98 percent) [1]. Throughout history and across the world, groundwater has played a crucial role as a primary source of water to support human life. The utilization of this resource has been subject to a substantial increase over the past century [2]. Indeed, groundwater is an excellent alternative source of potable water due to its reduced treatment fees. However, increasing water demand and projected climate change impacts on water resources are expected to raise the domestic and agricultural over-reliance on groundwater, also the availability and management of water supplies [3] [4]. In Africa, aquifers are becoming the primary source of domestic water supply and use for agriculture [5]. Despite this fact, there is a lack of quantitative data on groundwater resources in Africa, and groundwater storage is often excluded from evaluations of freshwater availability [6]. The delineation (mapping) of groundwater potential zones (GWPZs) is the ideal compromise where both the availability of surface sources and the financial affordability are extremely challenging [7]. It offers many benefits for water resource management, in particular, it aids in pinpointing optimal locations for groundwater well drilling, facilitates strategic planning for groundwater resource surveys, and establishes protective perimeters around the groundwater potential areas (zones), forming a basis for sustainable water management databases. Several authors, in recent decades, have focused their studies on groundwater potential zones mapping by emphasising the application of Geographical Information System (GIS) and Remote Sensing (RS) technology as an efficient method for delineating the potential zone [8]-[10] since the traditional techniques used to identify, delineate and map groundwater potential zones are based on costly and time-consuming geological, geophysical, and hydrogeological ground surveys [11]. A range of advanced mapping techniques have emerged over time to improve the understanding of groundwater distribution and management. From the earlier research, the Multi-Criteria Decision Making (MCDM) using Analytical Hierarchical Process (AHP) is an excellent decision-making method for problems with an overwhelming number of influencing factors [12]-[14]. On the other hand, the Artificial Neural Network (ANN), an increasingly popular machine learning technique [15] which has shown an international growing interest in recent years. MCDM techniques are numerical algorithms that define the suitability of a particular solution based on input and weighting criteria with mathematical and/or logical means to determine trade-offs in case of conflicts [9], while an ANN is described as a computational mechanism capable of acquiring, representing, and computing a map-

ping from one multivariate space of information to another, given a set of data representing that mapping [16]. This research first in West-Africa, aims to compare the effectiveness of RS combined with artificial intelligence and multicriteria analysis in mapping groundwater potential zones, providing valuable insights into groundwater resource assessment. In fact, using multiple methods to investigate a phenomenon produces more robust and convincing results than single-method studies [17]. Located in an area where water resources are limited and crucial for agriculture and domestic supply, the Sissili sub-catchment of Burkina Faso serves as an ideal setting to test the effectiveness of combined methods. Firstly, the work focus on identifying and understanding the parameters that contribute to groundwater potential. Secondly, it entails the detailed mapping and reclassification of parameters. Thirdly, it centres on refining and applying Artificial Neural Networks (ANN) and Analytical Hierarchy Process (AHP) methodologies to delineate groundwater potential zones in the sub-catchment. Finally, the study conducts a comprehensive comparison of the different resulting maps obtained.

2. Study Area and Data

2.1. Study Area

This study focuses on the Sissili sub-basin, located in Burkina Faso (**Figure 1**) shaped like a triangle, it covers an area of 7559 km^2. The sub-catchment hydrology is strongly influenced by the altimetry ranging between 281 - 451 m. The Sissili River flows across a relatively monotonous plateau, with little relief and a slight incline from north to south: the river's course which is oriented North-South between Thyou and Tabou, becomes North-West-South-East between Tabou and the Ghana border. From a morphological point of view, the Sissili watershed can be divided into two distinct sections: a northern part with little contrasting relief with abundant lateritic cuirasses hiding a bedrock that only rarely outcrops; a second part in the southern section with decapitated cuirasses leaving only witness mounds with numerous granite domes. This phenomenon is attributed to the regressive erosion of the river [18]. The sub-catchment encountered formations display geological diversity and can be classified into two primary geological groups from the Proterozoic era: the plutonic and the sedimentary volcano group. The aquifer system is typically developed within a weathered and fractured basement context. It is composed of three primary layers: a superficial lateritic cover, an intermediate saprolite zone and a deeper fissured that extends to the basement. Climatically, the region experiences two (2) distinct seasons: a dry season from November to April and a rainy season from May to October. The Sissili sub-basin has two climates: a Sudanian-type climate (southern Sudanian) located south of parallel 11˚30'N and a northern Sudanian-type climate. Annual precipitation averages over 900 mm, with a rainy season that lasts more than 6 months of the year (**Figure 2**). However, rainfall has been on a decreasing trend over the last two decades and there are slight fluctuations in annual temperatures [19]. The temperature has an average of 28˚C (**Figure 3**), with highest temperature occurring between March and April.

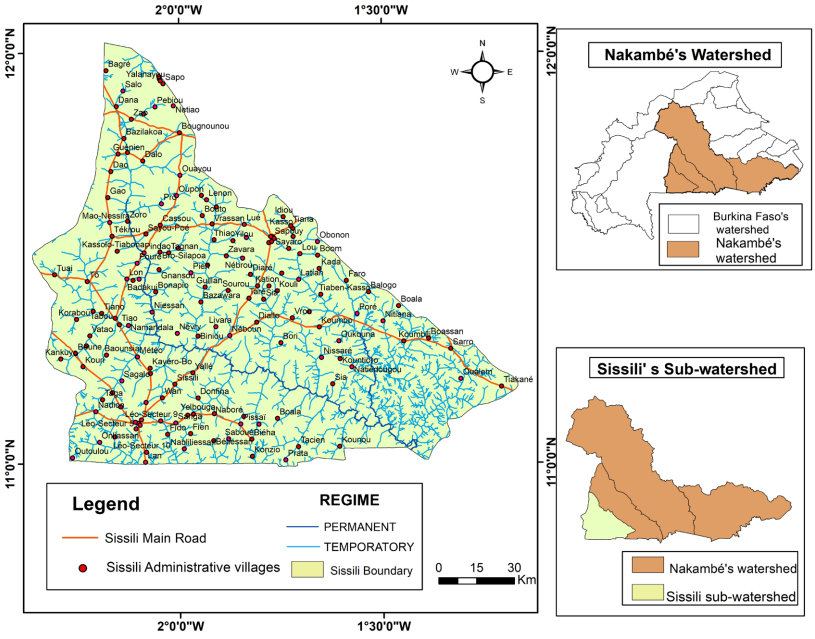

Figure 1. Sissili sub-catchment location.

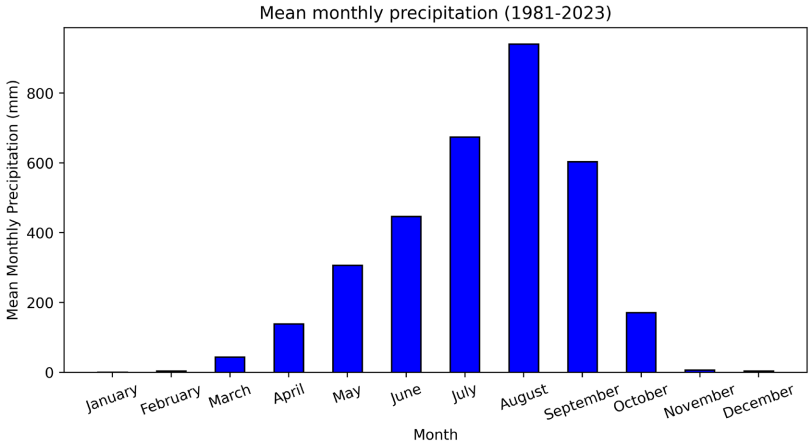

Figure 2. Mean monthly precipitation.

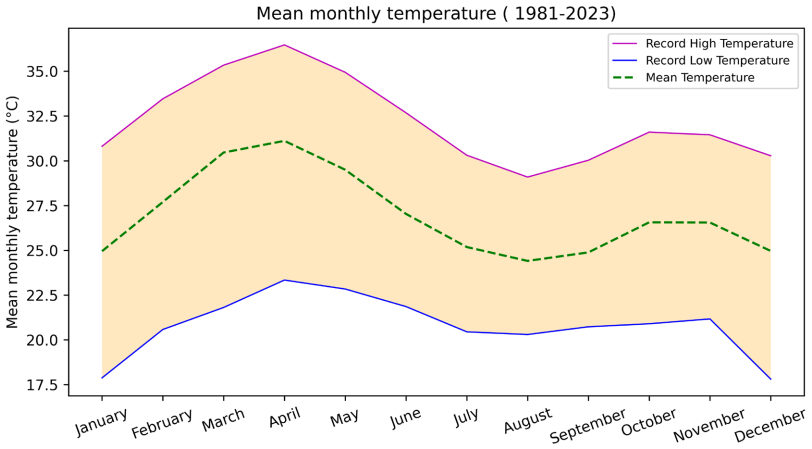

Figure 3. Mean monthly temperature.

2.2. Data

Several authors such as [20]-[23] have highlighted the key parameters best suited for delineating groundwater potential zones in a crystalline context. Numerous studies and research findings have also identified parameters that provide a comprehensive understanding of drilling productivity in a crystalline context in Burkina Faso [18] [24]. Based on the previous research, a detailed analysis was carried out on various variables, to identify groundwater potential zones in the sub-basin. These variables were derived from a combination of Remote Sensing data, topographic maps, and borehole information. Nine (9) key variables were considered including lithology, geology, lineament density, soil type, drainage density, borehole depth, land use patterns, Topographic Wetness Index (TWI), and efficient seepage. This integrated approach aims to offer a comprehension understanding of groundwater dynamics within the Sissili sub-catchment by employing tools such as ArcGIS, QGIS and R. ArcGIS and QGIS software were used for spatial data compilation, analysis, and visualization, while R was used for ANN models building and validation. Also, a total of 256 boreholes were selected based on the availability of reliable data, such as verified geographic coordinates and discharge values. A 5 × 5 km grid was applied over the study area to ensure a spatially balanced distribution covering the different lithological and hydrological zones of the sub-basin. In each grid cell containing data, a representative borehole was retained. This integrated methodology allowed both an assessment of spatial heterogeneity and the consideration of practical constraints related to data availability. Data from various sources were collected, processed, and integrated to delineate the GWPZs. **Table 1** resumes all the data sources and resolutions.

Table 1. The selected parameters, sources, and scale.

No.	INPUT	SOURCES	SCALE/RESOLUTION
1	Geology	BUMIGEB (Bureau des Mines et de la Géologie du Burkina) (February 2023)	1/200 000
2	Drainage density	Derived from ALOS PALSAR DEM	12.5 m × 12.5 m
3	Topographic Wetness Index	Derived from ALOS PALSAR DEM	12.5 m × 12.5 m
4	Land Use/Land Cover	ESAWORL (https://esa-worldcover.org/en)	10 m × 10 m
5	Soil	BUNASOLS (Bureau National des Sols)	500 m
6	Lithology	BUMIGEB (Bureau des Mines et de la Géologie du Burkina) (February 2023)	1/200 000
7	Efficient seepage	Derived from Climate Hazards Group InfraRed Precipitation with Station data (CHIRPS)	0.05˚ × 0.05˚
8	Boreholes depth	BUMIGEB (Bureau des Mines et de la Géologie du Burkina) (February 2023)	30 m × 30 m
9	Lineament density	Derived from ALOS PALSAR DEM	30 m × 30 m
10	Boreholes yield (for validation)	DGRE (Direction Générale des Ressources en Eau)	-

3. Methods

The nine (9) parameters were all processed within a GIS environment to ensure a uniform spatial resolution. The RS provided high-resolution data that was essential for characterizing the topography, drainage density and land cover.

3.1. An evaluation of the Primary Factors Influencing Groundwater Potential Zones

The identification of groundwater potential areas in the sub-basin is carried out by taking into account the main factors (parameters) influencing the recharge process and groundwater occurrence. They were selected based on an extensive literature assessment and for their direct impact on groundwater presence, replenishment, storage, and flow. Each factor affects groundwater potential by exerting differing degrees of influence.

Lithology: The occurrence and flow of groundwater are significantly influenced by the type of rocks, their structural characteristics, and their hydrological properties [11].

Geology: Geology affects the groundwater recharge by controlling the percolation of water [10]. Following rasterization, the data were categorized into eight (8) geological classes and five (5) lithological classes.

Efficient seepage: Rainfall is an essential factor in defining groundwater potential zones. It is, in fact, the primary source of natural recharge that develops groundwater resources [25]. CHIRPS satellite rainfall data for the year 2023 were used in this study, due to the strong correlation (85%) between CHIRPS data and observed rainfall data, and the limited availability of observational data in the study area. The Thornthwaite method has been applied in Excel to estimate the seepage water, which represents the portion of rainfall that infiltrates the subsurface and contributes to groundwater recharge. The efficient seepage is calculated based on climatic parameters and the usable ground reserve (RFU), using the Equation (1) below:

$$Q_{seep} = P - Q_R - AET - RFU \quad (1)$$

Where Q_{seep} represents the rainfall seepage water, Q_R is surface runoff, P the precipitation, AET is actual evapotranspiration, and RFU refers to the usable water in the ground, sourced from BUNASOLS (Source: Thornthwaite method).

Lineament density: The lineaments were extracted by multi-software processing of ALOS PALSAR data through firstly principal component analysis (PCA), followed by application of directional filter SOBEL on 0, 45, 90, and 135 degrees. Then manual lineament extraction has been processed. The lineaments have then been validated on the field. A lineament density (km/km^2) map has been prepared using the line density tool of spatial analysis tool of QGIS software, following the Equation (2) below:

$$Df = \frac{\sum_{i=1}^{n} L_i}{A} \quad (2)$$

Df = lineament density [km/km^2]; L_i = total length of lineament in km,

A = Area occupied by fractures in km².

Drainage density: Drainage density is the total length of the river system per unit of watershed area [26]. Using the ArcHydro tool of ArcGIS, individual drainage networks were extracted and delineated from the derived Digital Elevation Model (DEM). The equation (3) below allows the computing of the drainage density value in km/km².

$$\mathrm{D}d = \frac{\sum_{i=1}^{n} L_i}{A} \tag{3}$$

Dd = drainage density [km/km²]; Li = total length of the drainage network in km; A = Area considered in km².

Land use/land cover (LULC): LULC plays a crucial role in groundwater recharge [11]. The Land Use/Land Cover (LULC) map has been derived from ESAWORL (https://esa-worldcover.org/en) and has a resolution of 10 m × 10 m.

Soil: The medium through which water must penetrate to reach the water table is soil, which is an important factor in groundwater recharge and discharge [27]. The country soil data available is collected from BUNASOLS.

Borehole depth: The shallow depth indicates the high-water table inside the area while a deep depth represents challenges in terms of accessing its water resources [28].

Topographic Wetness Index (TWI): The Topographic Wetness Index (TWI) serves as a valuable tool for identifying groundwater potential through the analysis of spatial variations in soil moisture [20]. The calculation of TWI is based on the following Equation (4):

$$\mathrm{TWI} = \ln \frac{\alpha}{\tan \beta} \tag{4}$$

where α is Upslope contributing area and β Topographic gradient (Slope).

Borehole yield: The high value of borehole yield indicates that the area has favorable hydrogeological conditions for groundwater exploitation [28]. This parameter will serve to validate the different results obtained.

3.2. Analytical Hierarchy Process Model Development

The impact of various factors on the productivity of boreholes was assessed using weighted values, with the weighting approach based on expert opinions used in previous work [29] [30] carried out in the basement region. The scores from previous studies were used to assign weights to the factors in the current study. A common interval of 1 to 10 is used where the most favourable class for groundwater potential was assigned a score of 10, and the least favourable class was given a score of 1 based on [31] scale during the comparison between the parameters selected. The various factors were then compared pair-wise to create square matrices, from which the weighting coefficients were derived using the eigenvectors of these factors. The approach described by [32] was employed in this investigation. To reduce the subjectivity all parameters were normalized and reclassified., as they were measured on different scales and units. The pair-wise comparison

establishes the relative importance of each factor by comparing them two at a time. [14] demonstrate that a layer, with a high-weight parameter, can greatly affect the groundwater potential while a layer, with a low-weight parameter tends to have only a minor impact. The relative comparison importance of each parameter was determined using Saaty's scale as shown in Table 2.

Table 2. Saaty's scale explanation.

Intensity of Importance	Definition	Explanation
1	Equal importance	Two elements contribute equally to the objective
3	Moderate importance	Experience and judgment slightly favour one element over another
5	Strong importance	Experience and judgment slightly favour one element over another
7	Very strong importance	One element is favoured very strongly over another, its dominance demonstrated in practice
9	Extreme importance	The evidence favouring one element over another is of the highest possible over of affirmation
2, 4, 6, 8	Intermediate value	Can be used to express intermediate values
1/3, 1/5, 1/7, 1/9	Value of inverse comparison	-

All the thematic maps were integrated using the ArcGIS spatial analysis tool (Weighted Overlay Index (WOI) method) to generate a map depicting the groundwater potential zone. The final weights for all parameters were determined through the following steps using the following Equations (5)-(10).

1) The sum of the values in each column of the pair-wise comparison matrix:

$$L_{ij} = \sum_{i=1}^{n} C_{ij} \tag{5}$$

Where, L_{ij} is the total column value of the pair-wise comparison matrix and C_{ij} is the criteria used for analysis, such as drainage density, elevation and slope.

2) Normalized pair-wise comparison matrix:

$$X_{ij} = \frac{C_{ij}}{\sum_{n=1}^{n} C_{ij}} \tag{6}$$

X_{ij} represents the normalized pair-wise comparison matrix.

3) Standard Weight:

$$W_{ij} = \frac{\sum_{j=1}^{n} X_{ij}}{N} \tag{7}$$

W_{ij} = Standard Weight and N = number of criteria/parameters.

4) Consistency vector values:

$$\lambda = \sum_{i=1}^{n} CV_{ij} \tag{8}$$

Where λ is the Consistency vector.

5) The Consistency Index (CI) used as a degree of consistency:

$$CI = \frac{\lambda - n}{n - 1} \tag{9}$$

where CI = Consistency Index and n = Number of criteria.

6) Consistency ratio (Cr):

$$Cr = \frac{CI}{RI} \tag{10}$$

RI = Random Inconsistency (summarizes in Table 3). If the Consistency ratio is less than or equal to 0.10, then, the inconsistency is acceptable.

Table 3. Randomly index consistency.

No.	1	2	3	4	5	6	7	8	9
Random Consistency Value	0	0	0.58	0.9	1.12	1.24	1.32	1.41	1.45

3.3. Artificial Neural Model Development

The Artificial Neural Networks (ANN) are among the most commonly employed methods in machine learning algorithms [33] [34] and their application in water resources management, utilization, and modelling is increasingly common [35]. ANNs are beneficial because they can model complex data relationships, allowing the network to generalize and make predictions on new inputs without assuming a specific data distribution [36]. In this study, the ANN model was built using R software scripts. The process of using ANN for groundwater potential mapping involves several key stages. The design and configuration of the ANN model involve the inclusion of a suitable number of inputs, hidden and output layers. In the initial stages, groundwater potential parameters (data) have been obtained from a variety of sources, and for the current study, the same parameters selected for the multicriteria analysis have been used. All in all, 256 boreholes locations were used. The collected data have been then pre-processed to detect and correct any inconsistencies or errors that may have occurred. Then, the pre-processed data were randomly partitioned, seventy-five per cent (75%) into training while the remaining twenty-five per cent (25%) into testing datasets. The former is used to set or calibrate the ANN model and the latter to validate (test) its accuracy. As a dependent variable, the borehole yield was reclassified for the study area using scientific and objective criteria suggested by the Comité Interafricain d'Etudes Hydrauliques (CIEH). Groundwater suitable area training dataset was made up for areas where borehole yield was greater than 2.5 m^3/h, and a non-suitable area dataset was built up for areas where borehole yield was less than 2.5 m^3/h. The zonal statistics mean tool in QGIS was employed to compute the average value of a parameter within designated zones. This study utilized borehole yield locations as sites to derive the average values of nine (09) important parameters: lithology, geology, lineament density, soil type, drainage density, borehole depth, land use patterns, Topographic Wetness Index, and effective seepage. This approach allowed the evaluation of spatial distribution and relationships of these elements. The chosen neural network (NN) structure is a Multi-Layer Perceptron (MLP) that comprises three layers. The initial layer served as the input layer, with its nodes representing thematic maps of the nine (9) parameters influencing groundwater conditions in the Sissili catchment area. The second layer corresponds to

the internal or "hidden" layer with five (5) nodes, while the third layer functions as the output layer, responsible for presenting the output data with one (1) output node. This output data contains information regarding groundwater potential areas, which serve as the training sites for the model. Within the hidden layer, every node is interconnected with nodes in both the preceding and following layers through weighted connections. The architecture of the Artificial Neural Network (ANN) was optimized through manual hyperparameter tuning and cross-validation. Using the back-propagation training algorithm, the weights of each factor can be determined through the method defined by [37]. The backpropagation algorithm optimizes its weights and biases, to minimize the disparity between the predicted and actual groundwater potential values. It can incorporate multiple hidden layers, which empower the network to conduct various levels of processing and computation. Subsequently, the validated ANN model has been employed to generate the groundwater potential zone map. The area under the Receiver Operating Characteristic (ROC) and the Area Under Curve (AUC), which are generally used as statistical criteria for validating machine learning models were used to evaluate the predictive capability of the proposed model [38].

4. Results

4.1. Description of Selected Parameters

The nine (9) parameters selected such as Topographic Wetness Index, geology, effective seepage, lithology, lineament density, soil type, land use/land cover patterns, drainage density and borehole depth to delineate GWPZs were mapped and analyzed as described in the following **Figures 4-13**.

4.1.1. Geology

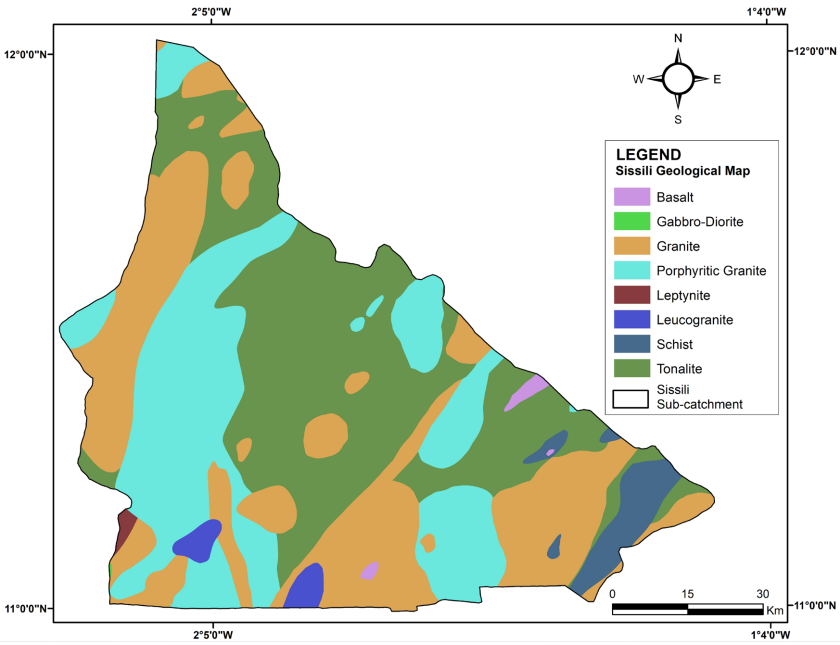

Figure 4. Geological map.

Geology affects the groundwater recharge by controlling the percolation of water flow [10]. The geological map of the study area displays eight distinct geological units, primarily consisting of tonalite and granite, which are conducive to infiltration (**Figure 4**). Tonalite, with low potentiality is widely represented and centred in the sub-basin, while the basalt with very low groundwater potential is less important in the sub-basin.

4.1.2. Lithology

Figure 5 describes the lithology of Sissili sub-catchment which is obtained from the BUMIGEB. The dominant lithologies observed are the migmatitic and anatectic gneiss which are not favourable for groundwater infiltration. The lithology with moderate groundwater potential, less represented in the sub-basin, is paragneiss.

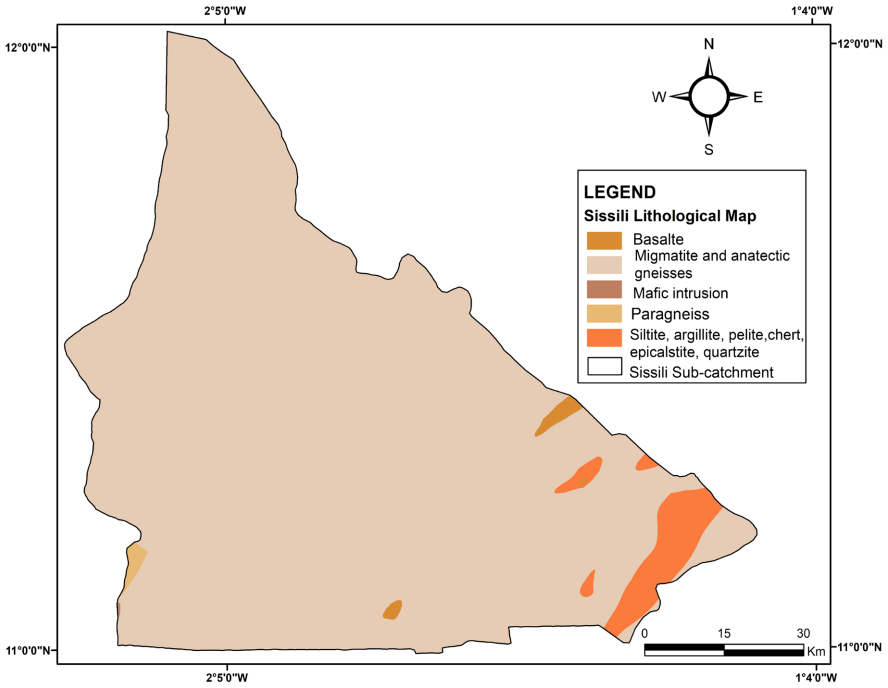

Figure 5. Lithological map.

4.1.3. Lineament Density

The term "lineament" refers to the linear elements of a landscape visible in satellite and aerial photography, mostly having a geological origin [26]. **Figure 6** presents the lineament density map and reveals a prevalence of moderate lineament density, characterized by values ranging from 0.032 to 1.79 km/km^2. High lineament density is favourable to infiltration while the low lineament doesn't favour water infiltration.

4.1.4. Drainage Density

The drainage density is an inverse function of permeability. An area with a low permeable surface tends to have high drainage density. As a result, high drainage

density implies low groundwater potential [25]. The resulting map illustrates in Figure 7, four major density classes ranging from 0 - 1.6 km/km^2, with high densities around rivers and at tributary crossings, decreasing as one moves away from rivers.

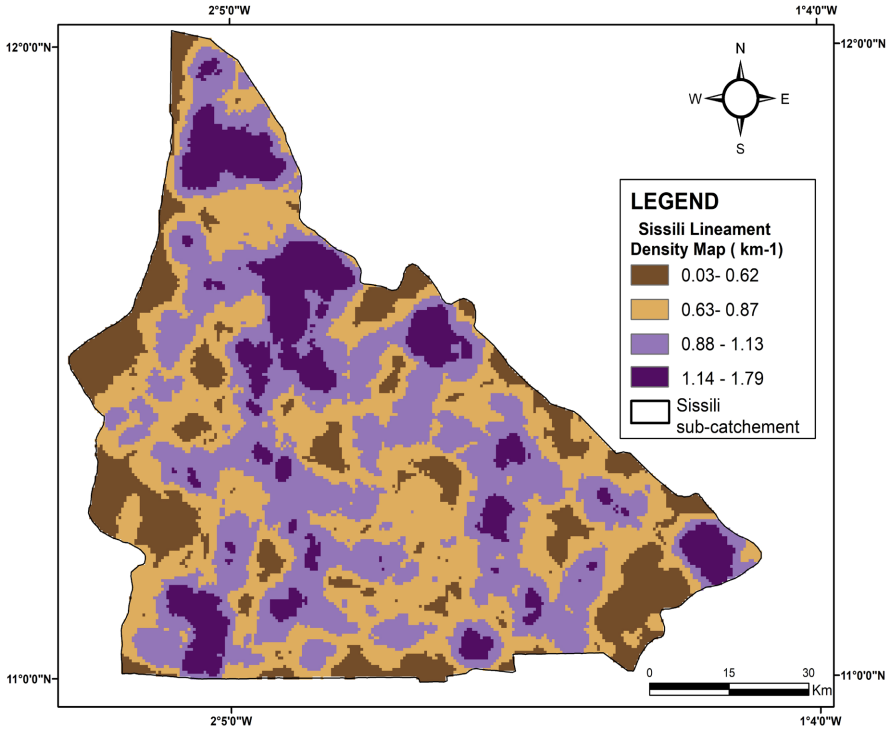

Figure 6. Lineament density map.

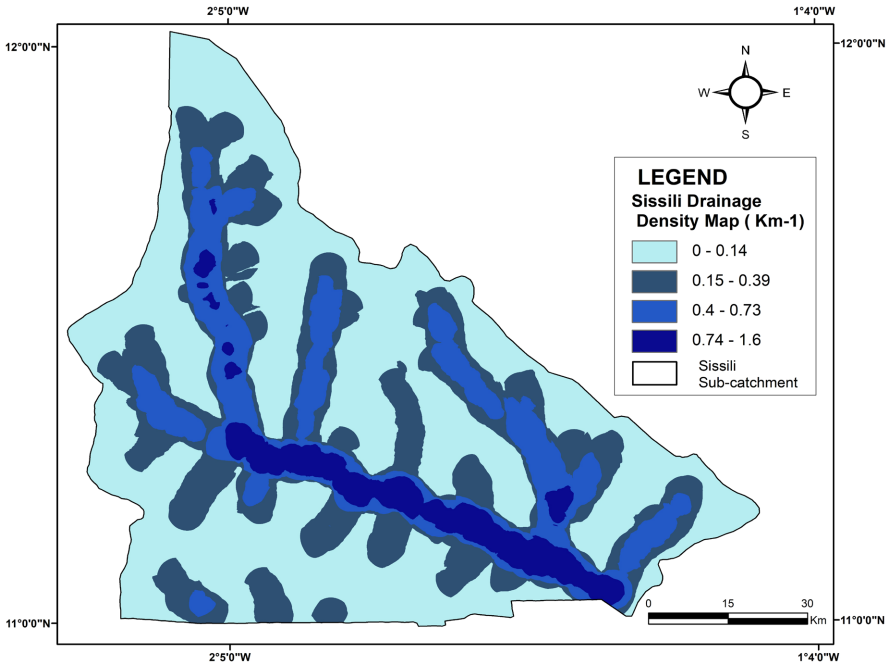

Figure 7. Drainage density map.

4.1.5. Efficient Seepage

Figure 8 represents the efficient seepage map in the sub-basin, ranging from 37 - 70 mm. The efficient seepage contributes to the recharge of aquatic environments and water tables. This is assumed to be the amount of rainfall that penetrates the aquifer. The southern part of the Sissili sub-catchment is the region with the highest infiltration portion.

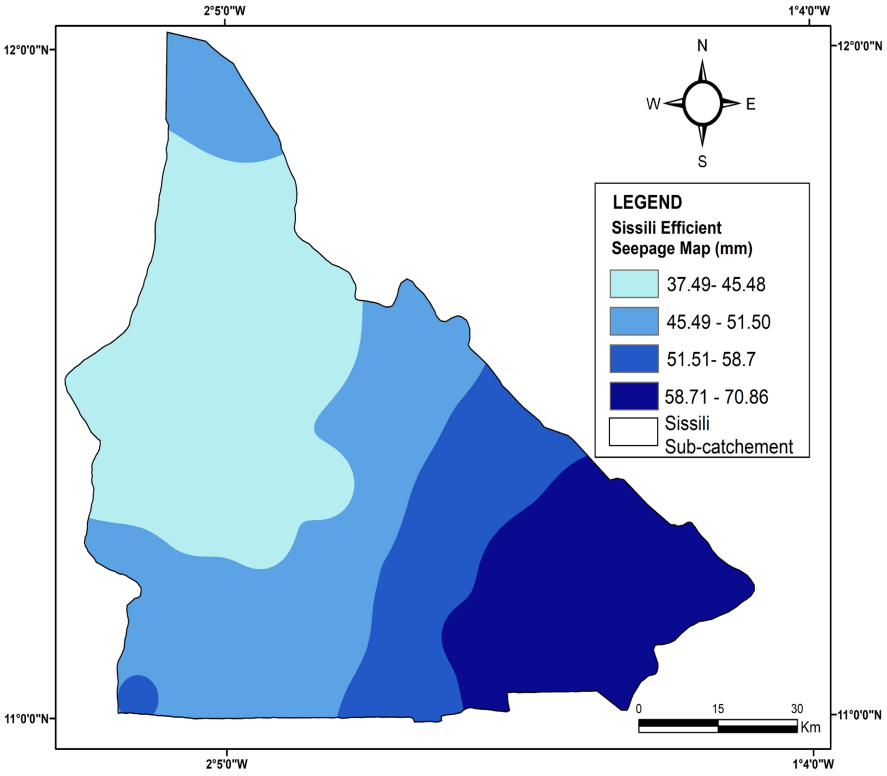

Figure 8. Efficient seepage map.

4.1.6. Land Use/Land Cover

The various forms of land use patterns that have been identified (Figure 9) in the sub-basin are primarily trees, grass, agricultural land, crops, and built-up. As the sub-basin is located in a predominantly rural area, the main land use is agricultural (crop) which has a low water infiltration. The built-up constructions also decrease water infiltration, whereas vegetation and water bodies increase water penetration into aquifers through the confinement of water in the soil, thus avoiding direct evaporation [39].

4.1.7. Boreholes Depth

The depth of the boreholes is presented in Figure 10 with values ranging from 35 to 99 m. This range indicates that majority of the boreholes have been realized based on deep depth which is synonymous with limited groundwater availability. This result shows that mainly areas close to the southern Ghanaian border are favourable to water infiltration (shallow depths).

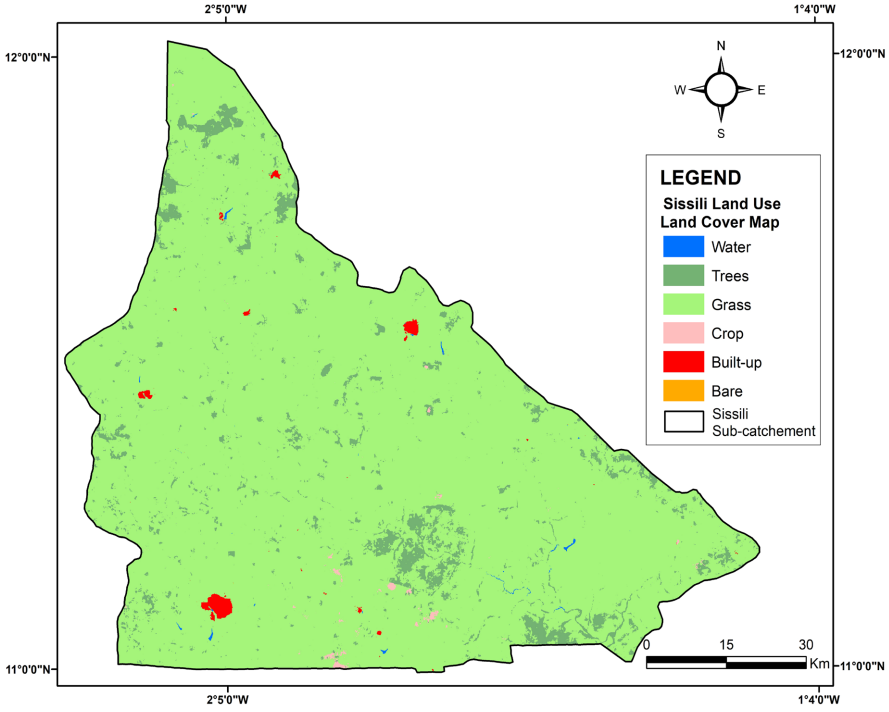

Figure 9. Land Use/Land Cover map.

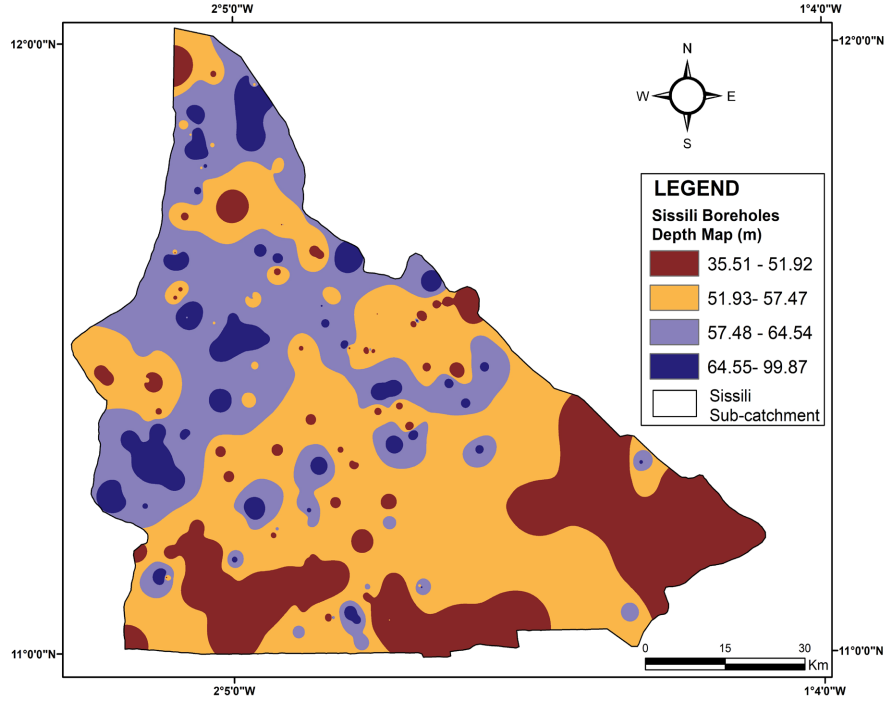

Figure 10. Boreholes depth map.

4.1.8. Topographic Wetness Index (TWI)

The Topographic Wetness Index (TWI) values obtained are ranked between 7.3 and 26.32 as presented in **Figure 11**. Greater TWI values correspond to reduced slopes, thereby facilitating a greater potential for groundwater accumulation.

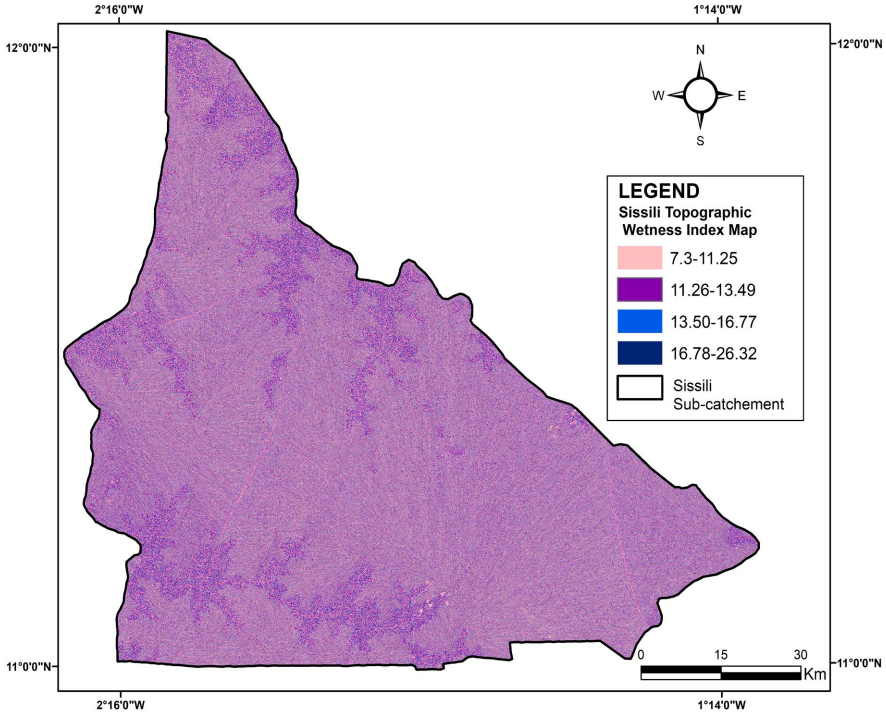

Figure 11. Topographic wetness index map.

4.1.9. Soil

The soil map obtained in **Figure 12** classifies the three main soil categories into hydromorphic, raw mineral, and poorly developed soils. Each class is characterized by its role in groundwater accumulation. Raw mineral and poorly developed soils are present in relatively small areas and it is highly resistant to recharge because of its low permeability.

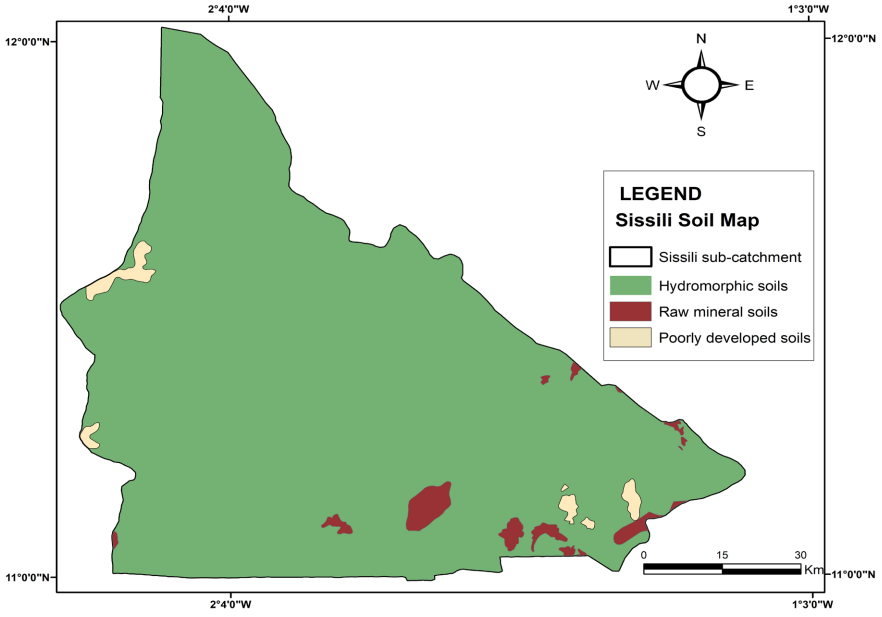

Figure 12. Soil map.

4.2. Reclassification of Parameters and Pair-Wise Comparison

The different selected parameters have been reclassified, and each parameter class have been allocated a weigh and a normalized weight to prepare the groundwater potential map. The following Table 4 summarizes the criteria and sub-criteria ranges.

Table 4. Criteria and sub-criteria ranges for groundwater potential assessment.

Factor	ID	Class	Contribution to groundwater infiltration	Allocated Weight	Normalized Weight (%)
Geology	1	Basalt	Very Low	1	11
	2	Gabbro-Diorite	Low	3	
	3	Granite	Very Low	1	
	4	Porphyritic Granite	Low	3	
	5	Leptynite	High	7	
	6	Leucogranite	Moderate	5	
	7	Schist	Very High	10	
	8	Tonalite	Low	3	
Lithology	1	Basalt	Very Low	1	18
	2	Migmatite and anatectic Gneiss	Low	3	
	3	Malfic intrusion	Low	3	
	4	Paragneiss	Moderate	5	
	5	Siltite, Argillite pelite, Chert, Epicalstite quartzite	Low	3	
Drainage Density	1	0 - 0.32	Very High	10	11
	2	0.33 - 0.64	High	7	
	3	0.65 - 0.97	Moderate	5	
	4	0.98- 1.29	Low	3	
	5	1.30 - 1.61	Very Low	1	
Efficient Seepage	1	37.49 - 45.31	Very Low	1	10
	2	45.34 - 50.97	Very Low	1	
	3	50.98 - 57.51	Low	3	
	4	57.52 - 63.4	Low	3	
	5	63.41 - 70.86	Low	3	
Soil Texture	1	Hydromorphic soil	Low	3	11
	2	Raw minerals soil	Very Low	1	
	3	Poorly developed soils	Very Low	1	
TWI	1	7.30 - 11.10	Very Low	1	12
	2	11.11 - 12.74	Low	3	
	3	12.74 - 14.84	Moderate	5	
	4	14.85 - 17.81	High	7	
	5	17.82 - 26.32	Very High	10	

Continued

Land Use/Land Cover	1	Water	Very High	10	9
	2	Forest	High	7	
	3	Grass	Moderate	5	
	4	Crop (agriculture)	Low	3	
	5	Built-up	Very Low	1	
	6	Bare land	Low	3	
Boreholes' depth	1	35.51 - 50.15	Very High	10	11
	2	50.16 - 55.19	High	7	
	3	55.2 - 59.99	Moderate	5	
	4	59.99 - 67.31	Low	3	
	5	67.31 - 99.87	Very Low	1	
Lineament Density	1	0.01 - 0.39	Very Low	1	7
	2	0.40 - 0.77	Low	3	
	3	0.77 - 1.15	Moderate	5	
	4	1.16 - 1.53	High	7	
	5	1.54 - 1.90	Very High	10	

4.3. Weighting, Scoring, and Index Calculation of the Extracted Parameters

Table 5 presented below displays the normalized pair-wise matrix assigned to each thematic layer throughout the process of pair-wise comparison. A square matrix was utilized to conduct a pair-wise comparison of all input parameters, with the diagonal components consistently set to 1. The calculation of the normalized pair-wise matrix using Equation (6).

Table 5. Normalized pair-wise matrix.

Matrix	Lithology	Geology	Soil	LULC	TWI	Drainage density	Efficient seepage	Lineament density	Boreholes' depth	Normalized Principal Eigenvector
Lithology	1	7/5	5/2	7/5	5/2	7/4	7/4	3	1	17.84%
Geology	5/7	1	1	4/7	4/5	7/4	7/5	2	1	11.25%
Soil	2/5	1	1	7/5	7/4	4/7	7/5	7/5	1	10.91%
LULC	5/7	4/7	5/7	1	4/5	4/7	1/3	2	1	9.70%
TWI	2/5	5/4	4/7	5/4	1	7/5	2	22/9	1	11.91%
Drainage density	4/7	4/7	7/4	7/4	5/7	1	7/5	7/4	1	11.33%
Efficient seepage	4/7	5/7	5/7	3	1/2	5/7	1	1	1	10.05%
Lineament density	1/3	1/2	5/7	1/2	2/5	4/7	1	1	1	6.55%
Boreholes' depth	1	1	1	1	1	1	1	1	1	10.46%

4.4. Groundwater Potential Zones (GWPZs)

The output from the AHP final map obtained was classified into areas of very low,

low, moderate, high, and very high groundwater potential zones. The results were validated using the borehole yield data collected. Figure 13 gives the final map of the groundwater potential zones obtained.

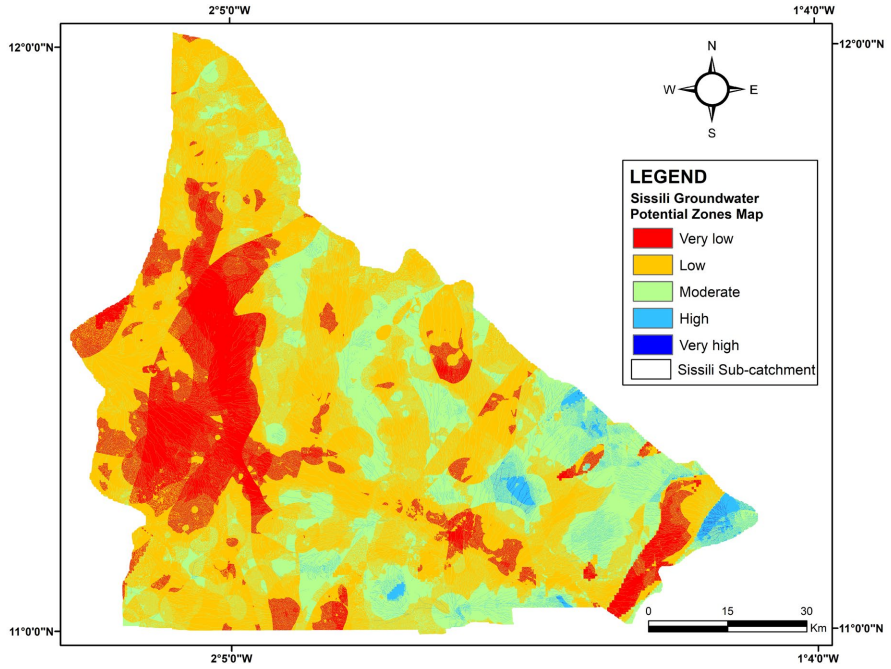

Figure 13. Sissili groundwater potential zone map using AHP.

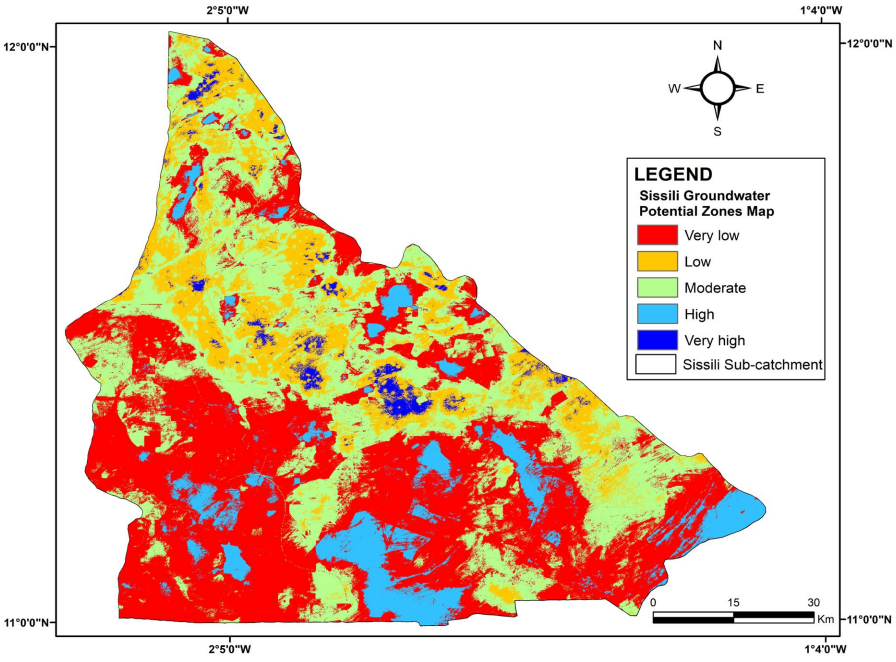

Figure 14. Groundwater Potential Zone map using ANN.

The final map of the ANN process was categorized into zones of very low, low, moderate, high, and very high groundwater potential. The results were corrobo-

rated using the yield data from the drilled wells, as well as the AUC and ROC obtained post-analysis. Figure 14 represents the groundwater potential zone map obtained.

4.5. Validation of the GWPZs

The verification of the reliability of a model's output is necessary before utilizing the obtained results. Consequently, yield data from seventy-eight (78) existing boreholes were used to validate the delineated GWPZs ranging from 0.51 to 12.9 m^3/h, with an average of 2.55 m^3/h. To assess the degree of accuracy of the AHP process, the Consistency Index (CI) and the Consistency ratio (Cr) have been calculated based on the previous equations (9) and (10). The Eigenvector technique was used to calculate the principal Eigenvalue (λ) through the formula (8) where $\lambda_{max} = 9.56$. The Cr = 0.048, which is less than or equal to 0.10, showing that the inconsistency is acceptable. As a result, boreholes situated in areas with very low exhibit a yield ranging between 1 - 2 m^3/h, and low groundwater potential exhibits a yield ranging between 2.1 - 5 m^3/h. boreholes located in areas with moderate groundwater potential exhibit a yield ranging from 5.1 to 10 m^3/h, while those in high and very high groundwater potential zones demonstrate yield superior to 10 m^3/h following the Comité Interafricain d'Etudes Hydrauliques (CIEH) classification. The AHP result shows 18% of boreholes fall within the very low groundwater potential zones while 29% of boreholes on the ANN map. In the low potential zone, 27% of boreholes lay in this class in AHP map while 16% of boreholes in ANN map. In the moderate potential zone maps obtained with AHP and ANN process, respectively 32% and 18% of boreholes are located in this class, while in the high potential zone class 15% and 22% of borehole, respectively are identified in this class. Finally, the very high groundwater potential class accounts

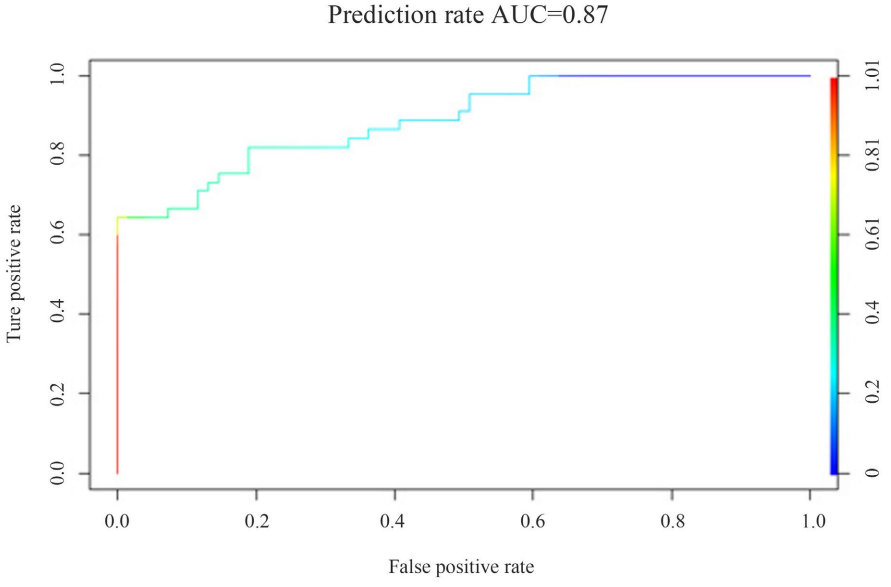

Figure 15. ANN prediction rate.

for 8% and 15% of boreholes in the AHP and ANN maps, respectively. Also, the Area Under Curve (AUC) has been calculated, generally used as statistical criteria for validating machine learning models to evaluate the predictive capability of the model. The ROC is quantitatively characterized by the AUC. In an ideal classifier (perfect model), the AUC equals 1, whereas for a random classifier (inaccurate model), it yields a value of 0.5 [40]. **Figure 15** displays the AUC of 0.87 while **Figure 16** shows the satisfactory performance result of 0.93.

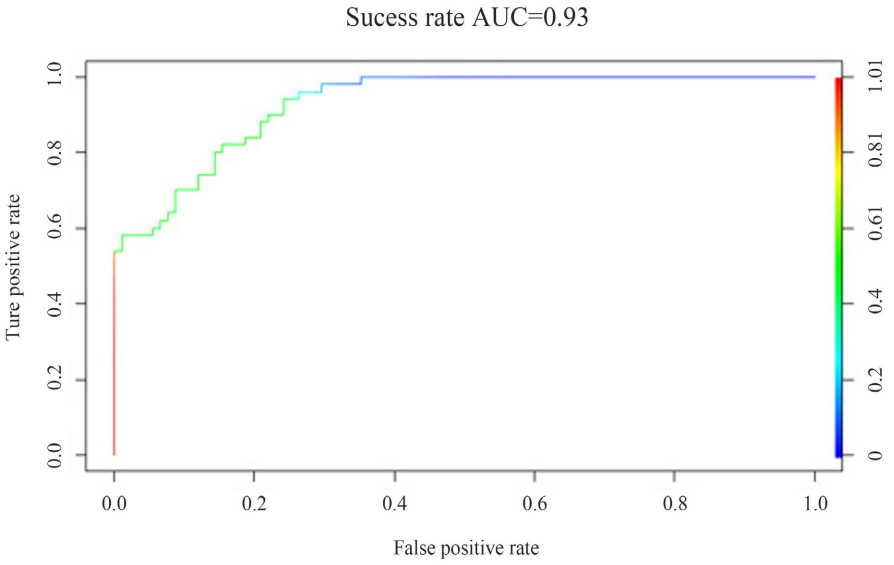

Figure 16. ANN success rate.

5. Discussion

Over the past 40 to 50 years, various anthropogenic activities and unbalanced development have significantly reduced groundwater recharge, even though groundwater remains a renewable resource. In this context, a better understanding of groundwater potential is essential to ensure sustainable development and effective strategic planning [20]. In Burkina Faso, few studies have focused on identifying high groundwater potential zones, even though the country's predominant basement complex generally stores less groundwater compared to sedimentary basins [28]. Therefore, accurately targeting areas with the highest potential is crucial to optimize borehole yields. For this purpose, Remote Sensing, GIS techniques, and Artificial Neural Networks (ANN) have been hence, used to assess groundwater potential zones. The integrated approach based on nine (09) factors identified five (05) distinct classes of groundwater potential. The AHP obtained map were organized into 5 categories: very low, low, moderate, high, and very high (as depicted in **Figure 13**) representing respectively 16.36% (1236.43 km^2), 51.53% (3895.39 km^2), 29.24% (2209.89 km^2), 2.82% (213.17 km^2) and 0.05% (4.12 km^2) of the entire area of the sub-basin. These results suggest a predominantly low potential (more than 50% of the total area), which could explain the high failure rate of drilling in this zone, as emphasized by [18] and [19]. The analysis from the ANN

approach also reveals five (5) classes (**Figure 14**), with a different breakdown: 43.56% (3292.98 km^2) of the area is classified as having very low potential, 14.60% (1103.82 km^2) as low, 31.10% (2350.86 km^2) as moderate, 9.10% (687.82 km^2) as high, and 1.63% (123.52 km^2) as very high. The high groundwater potential areas are located mainly in zones with high precipitation and high infiltration capacity. These zones coincide with those characterized by metamorphic rocks (gneiss) and volcanic formations (basalts, ignimbrites) known as having high potential [41]. These areas also often exhibit soils with low drainage, low altitude, high lineament density, high permeability, very high infiltration rates, and very low groundwater depth. Conversely, areas with low groundwater potential are located in the migmatite complex, characterized by sharp slopes and high drainage density. A comparison of the results obtained using the AHP and ANN methods reveals some notable differences, although there are some similarities. For example, some areas identified as having very low potential in AHP coincide with those identified as very low potential by ANN, even the ANN map display more area with low potential. Areas with low groundwater potential according to AHP coincide with low potential by the ANN even the surface of low-potential areas is more pronounced. Also, the areas considered as having high and very high groundwater potential in AHP correspond with some high and high potential area in ANN. Nevertheless, the discrepancy (area that not entirely coincide) can be explained by the methodological differences between the two approaches. AHP relies heavily on precise numerical judgments, which might be challenging in situations where emotions cloud decision-makers' judgments. Moreover, AHP fails to consider uncertainties and risks, and modifications to the criteria or available options can have a substantial impact on its outcomes [42]. On the other hand, ANN is capable of modelling non-linear relationships and complex spatial interactions, and can provide a more nuanced assessment of groundwater potential zones [43]. This could explain the higher classification of areas as having very low potential. Despite the high AUC (0.93), the large proportion of areas classified as "very low" potential aligns with field observations of low-yield boreholes. This outcome reflects the model's realistic performance rather than overfitting. According to [21], the predominance of low-potential zones in a basin is favoured by the thinness of the alteration mantle, which severely limits the storage function of the alterite aquifer, and the low fracture density which limits the infiltration or conductive function of basement aquifers. This explanation aligns with the low fracture density (0.032 to 1.79 km/km^2) and the alteration thickness ranging from (7 - 48 m) in the subcatchment. Furthermore, the validation process using the boreholes yield and AUC reveals that the ANN prediction map obtained gives more precise results. Hence, the areas identified as having high potential should be prioritized for establishing protection perimeters given the high risk of rapid transfer of contaminants to the aquifers, as highlighted by [19]. Additionally, these areas present opportunities for enhancing aquifer hydraulic potential, through artificial recharge, and could serve as a prime area for drilling. The methodologies employed by ANN and AHP are

relevant in regions such as the Sissili sub-catchment with limited access to field data, as they provide precise estimations based on remotely sensed and spatial data. However, the ANN method has demonstrated a more precise delineation of groundwater potential zones, particularly when validated against field data, ensuring a more reliable assessment of groundwater potential zones.

6. Conclusion

The research goals related to water availability have been carried out by taking into account the nine (09) main interdependent factors, that affect the groundwater infiltration process in a specific manner. After generating the thematic layers, the factors have been characterized using a descriptive scale based on their influence on water infiltration. In parallel, the Artificial Neural Network refines the characterization by normalizing and optimizing weights and biases through a backpropagation algorithm to identify groundwater potential zones. Considering the outcomes of this study, we can conclude on the following key points: the two different methods allowed a qualitative estimation of groundwater potential in the studied area. The final output map derived from AHP was classified into five (5) classes of groundwater potential zone (very low, low, moderate, high and very high) which respectively account 16.36%, 51.53%, 29.24%, 2.82% and 0.05% respectively. The ANN method shows the more accurate results which account respectively for 43.56%, 14.60%, 31.10%, 9.10%, and 1.63% of the entire sub-basin. This work is essential in pinpointing areas well-suited for groundwater protection and conservation efforts, aligning with the United Nation's Sustainable Development Goals (SDGs) 6, which aims to ensure sustainable management of water and sanitation for all. The findings can serve as valuable resources for decision-makers to promote sustainable groundwater utilization. However, it is crucial to acknowledge the limitations and weaknesses associated with the employed methodologies. Firstly, ANN models tend to demand a substantial amount of time for execution and impose a significant computing load. Secondly, addressing both continuous and discrete data within an ANN program presents a complex challenge. Lastly, the AHP method relies on specialist perception, introducing uncertainties that may arise from variations in weightage values. To enhance the precision of the forecasted groundwater potential map, the integration of factors such as geomorphology, evapotranspiration, and transmissivity could be helpful.

Acknowledgements

I express my gratitude to the Bureau des Mines et de la Géologie du Burkina (BUMIGEB), to the Bureau National des Sols (BUNASOLS), and to the Direction Générale des Ressources en Eau (DGRE) for supplying data and pertinent documents that facilitated my research.

Conflicts of Interest

The authors declare no conflicts of interest regarding the publication of this paper.

References

[1] Eileen, P., Fan, Y., Cherry, J., *et al.* (2020) Groundwater in Our Water Cycle.

[2] Jakeman, A.J., Barreteau, O., Hunt, R.J., Rinaudo, J.D. and Ross, A. (2016) Integrated Groundwater Management: Concepts, Approaches and Challenges. Springer, 1-762. https://doi.org/10.1007/978-3-319-23576-9

[3] Adelana, S.M.A. (2008) Groundwater Research Issues in Africa. 1-7.

[4] Taylor, R.G., Scanlon, B., Döll, P., Rodell, M., van Beek, R., Wada, Y., *et al.* (2012) Ground Water and Climate Change. *Nature Climate Change*, **3**, 322-329. https://doi.org/10.1038/nclimate1744

[5] Horváthová, E. (2022) Analysis of Drinking Water Treatment Costs—With an Application to Groundwater Purification Valuation. *One Ecosystem*, **7**, e82125. https://doi.org/10.3897/oneeco.7.e82125

[6] MacDonald, A.M., Bonsor, H.C., Dochartaigh, B.É.Ó. and Taylor, R.G. (2012) Quantitative Maps of Groundwater Resources in Africa. *Environmental Research Letters*, **7**, Article ID: 024009. https://doi.org/10.1088/1748-9326/7/2/024009

[7] Dibaba, W.T., Demissie, T.A. and Miegel, K. (2020) Watershed Hydrological Response to Combined Land Use/Land Cover and Climate Change in Highland Ethiopia: Finchaa Catchment. *Water*, **12**, Article No. 1801. https://doi.org/10.3390/w12061801

[8] Singh, S.K., Zeddies, M., Shankar, U. and Griffiths, G.A. (2019) Potential Groundwater Recharge Zones within New Zealand. *Geoscience Frontiers*, **10**, 1065-1072. https://doi.org/10.1016/j.gsf.2018.05.018

[9] Ali, I.A. and Konatã, M. (2020) Identification and Mapping of Groundwater Potential Recharge Areas in the Dosso Region (Southwestern of Niger). *European Scientific Journal*, **16**, 217-241. https://doi.org/10.19044/esj.2020.v16n18p217

[10] Ghute, B.B. and Md. Babar, S. (2020) An Approach to Mapping Groundwater Recharge Potential Zones Using Geospatial Techniques in Kayadhu River Basin, Maharashtra. *Indian Journal of Agricultural Research*, **55**, 23-32. https://doi.org/10.18805/ijare.a-5477

[11] Ahirwar, S., Malik, M.S., Ahirwar, R. and Shukla, J.P. (2020) Application of Remote Sensing and GIS for Groundwater Recharge Potential Zone Mapping in Upper Betwa Watershed. *Journal of the Geological Society of India*, **95**, 308-314. https://doi.org/10.1007/s12594-020-1430-3

[12] Chenini, I., Mammou, A.B. and El May, M. (2009) Groundwater Recharge Zone Mapping Using GIS-Based Multi-Criteria Analysis: A Case Study in Central Tunisia (Maknassy Basin). *Water Resources Management*, **24**, 921-939. https://doi.org/10.1007/s11269-009-9479-1

[13] Singh, P., Thakur, J.K. and Kumar, S. (2013) Delineating Groundwater Potential Zones in a Hard-Rock Terrain Using Geospatial Tool. *Hydrological Sciences Journal*, **58**, 213-223. https://doi.org/10.1080/02626667.2012.745644

[14] Morgan, H., Hussien, H.M., Madani, A. and Nassar, T. (2022) Delineating Groundwater Potential Zones in Hyper-Arid Regions Using the Applications of Remote Sensing and GIS Modeling in the Eastern Desert, Egypt. *Sustainability*, **14**, Article No. 16942. https://doi.org/10.3390/su142416942

[15] Tamiru, H. and Wagari, M. (2021) Evaluation of Data-Driven Model and GIS Technique Performance for Identification of Groundwater Potential Zones: A Case of Fincha Catchment, Abay Basin, Ethiopia. *Journal of Hydrology: Regional Studies*, **37**, Article ID: 100902. https://doi.org/10.1016/j.ejrh.2021.100902

[16] Garrett Jr., J.H. (1994) Where and Why Artificial Neural Networks Are Applicable in Civil Engineering. *Journal of Computing in Civil Engineering*, **8**, 129-130.

[17] Davis, D.F., Golicic, S.L. and Boerstler, C.N. (2010) Benefits and Challenges of Conducting Multiple Methods Research in Marketing. *Journal of the Academy of Marketing Science*, **39**, 467-479. https://doi.org/10.1007/s11747-010-0204-7

[18] Savadogo, A.N. (1984) Géologie et hydrogéologie du socle cristallin de Haute-Volta: Étude régionale du bassin versant de la Sissili. Université Scientifique et Médicale de Grénoble, 350.

[19] Faye, M.D. (2022) Caractérisation et modélisation du transfert de polluants dans un aquifère fracture en milieu de socle (Sous bassin versant de la Sissili-Burkina).

[20] Arulbalaji, P., Padmalal, D. and Sreelash, K. (2019) GIS and AHP Techniques Based Delineation of Groundwater Potential Zones: A Case Study from Southern Western Ghats, India. *Scientific Reports*, **9**, Article No. 2082. https://doi.org/10.1038/s41598-019-38567-x

[21] Haman, D.J.B., Fantong, F.W., Ewodo Mboudou, G.O.A. and Messi, G. (2022) Approche décisionnelle géospatiale et multicritère dans l'identification des zones potentielles de recharge des eaux souterraines: Cas du bassin versant du Mayo Bocki au Nord Cameroun. *Journal of the Cameroon Academy of Sciences*, **18**, 339-356. https://doi.org/10.4314/jcas.v18i1.5

[22] Ake, G.E., Kouame, K.J., Bénédicte, A. and Patrice, J. (2024) Cartography of Potential Recharge Areas of the Bonoua Aquifer (Southeastern Côte d'Ivoire). *Revue des Sciences de l'Eau*, **31**, 129-144.

[23] Jasechko, S., Seybold, H., Perrone, D., Fan, Y., Shamsudduha, M., Taylor, R.G., *et al.* (2024) Rapid Groundwater Decline and Some Cases of Recovery in Aquifers Globally. *Nature*, **625**, 715-721. https://doi.org/10.1038/s41586-023-06879-8

[24] Koussoube, Y. (1996) Hydrogéologie en milieu de socle cristallin du burkina faso.

[25] Tolche, A.D. (2020) Groundwater Potential Mapping Using Geospatial Techniques: A Case Study of Dhungeta-Ramis Sub-Basin, Ethiopia. *Geology, Ecology, and Landscapes*, **5**, 65-80. https://doi.org/10.1080/24749508.2020.1728882

[26] Shaban, A., Khawlie, M. and Abdallah, C. (2005) Use of Remote Sensing and GIS to Determine Recharge Potential Zones: The Case of Occidental Lebanon. *Hydrogeology Journal*, **14**, 433-443. https://doi.org/10.1007/s10040-005-0437-6

[27] Kaewdum, N. and Chotpantarat, S. (2021) Mapping Potential Zones for Groundwater Recharge Using a GIS Technique in the Lower Khwae Hanuman Sub-Basin Area, Prachin Buri Province, Thailand. *Frontiers in Earth Science*, **9**, Article ID: 717313. https://doi.org/10.3389/feart.2021.717313

[28] Yabre, S., Koussoubé, Y., Gaëtan, S.É.S., Yalo, N. and Silliman, S. (2023) Identification of Groundwater Potential Zones in Samendeni Watershed in Sedimentary and Semi-Arid Contexts of Burkina Faso, Using Analytic Hierarchy Process (AHP) Method and GIS. *American Journal of Climate Change*, **12**, 172-203. https://doi.org/10.4236/ajcc.2023.121009

[29] Koffi, K.M., Yao, K.T., Mobio, A. and Oga, Y.M.S. (2016) Apport de l'analyse multicritère à la cartographie des zones favorables à l'implantation de forages dans la région de Gagnoa (Centre-ouest de la Côte d'Ivoire). *Geo-Eco-Trop*, **40**, 327-344.

[30] Jourda, J.P., Kouame, K.J., Saley, M.B., Eba, L.E., Anani, A.T. and Biemi, J. (2015) Determination of Potentially Favorable Zones for the Setting up of Manual Boreholes from Multicriterion Analysis and GIS: Case of Cote d'Ivoire. *Journal of Water Science*, **28**, 119-137. https://doi.org/10.7202/1032294ar

[31] Saaty, T.L. (1977) A Scaling Method for Priorities in Hierarchical Structures. *Journal*

of Mathematical Psychology, **15**, 234-281.
https://doi.org/10.1016/0022-2496(77)90033-5

[32] Saaty, T.L. and Vargas, L.G. (1980) Hierarchical Analysis of Behavior in Competition: Prediction in Chess. *Behavioral Science*, **25**, 180-191.
https://doi.org/10.1002/bs.3830250303

[33] Olden, J.D., Joy, M.K. and Death, R.G. (2004) An Accurate Comparison of Methods for Quantifying Variable Importance in Artificial Neural Networks Using Simulated Data. *Ecological Modelling*, **178**, 389-397.
https://doi.org/10.1016/j.ecolmodel.2004.03.013

[34] Sokeng, V.-C.J., Kouamé, F.K., Ngounou Ngatcha, B., Dibi N'da, H., Akpa You, L. and Rirabe, D. (2016) Delineating Groundwater Potential Zones in Western Cameroon Highlands Using GIS Based Artificial Neural Networks Model and Remote Sensing Data Mapping of Groundwater Potentials in Western Cameroon Highlands: Contribution of Remote Sensing (Optical and Rad). *International Journal of Innovation and Applied Studies*, **15**, 747-759. http://www.ijias.issr-journals.org/

[35] Dtissibe, F.Y., Ari, A.A.A., Titouna, C., Thiare, O. and Gueroui, A.M. (2020) Flood Forecasting Based on an Artificial Neural Network Scheme. *Natural Hazards*, **104**, 1211-1237. https://doi.org/10.1007/s11069-020-04211-5

[36] Lee, S., Song, K., Kim, Y. and Park, I. (2012) Regional Groundwater Productivity Potential Mapping Using a Geographic Information System (GIS) Based Artificial Neural Network Model. *Hydrogeology Journal*, **20**, 1511-1527.
https://doi.org/10.1007/s10040-012-0894-7

[37] Cilimkovic, M. (2015) Neural Networks and Back Propagation Algorithm. Institute of Technology Blanchardstown, 15, 3-7.

[38] Hong, H., Liu, J., Zhu, A., Shahabi, H., Pham, B.T., Chen, W., *et al.* (2017) A Novel Hybrid Integration Model Using Support Vector Machines and Random Subspace for Weather-Triggered Landslide Susceptibility Assessment in the Wuning Area (China). *Environmental Earth Sciences*, **76**, Article No. 652.
https://doi.org/10.1007/s12665-017-6981-2

[39] Singh, S.K., Zeddies, M., Shankar, U. and Grif, G.A. (2018) Geoscience Frontiers Potential Groundwater.

[40] Hand, D.J. (2009) Measuring Classifier Performance: A Coherent Alternative to the Area under the ROC Curve. *Machine Learning*, **77**, 103-123.
https://doi.org/10.1007/s10994-009-5119-5

[41] Savadogo, N. (1975) Hydrogéologie du bassin versant de la Haute-Sissili (Haute-Volta).

[42] Karthikeyan, R., Venkatesan, K.G.S. and Chandrasekar, A. (2016) A Comparison of Strengths and Weaknesses for Analytical Hierarchy Process. *Journal of Chemical and Pharmaceutical Sciences*, **9**, 12-15. https://www.jchps.com

[43] Zaresefat, M., Derakhshani, R., Nikpeyman, V., GhasemiNejad, A. and Raoof, A. (2023) Using Artificial Intelligence to Identify Suitable Artificial Groundwater Recharge Areas for the Iranshahr Basin. *Water*, **15**, Article No. 1182.
https://doi.org/10.3390/w15061182